Since January 2020 Elsevier has created a COVID-19 resource centre with free information in English and Mandarin on the novel coronavirus COVID-19. The COVID-19 resource centre is hosted on Elsevier Connect, the company's public news and information website.

Pharmacological Research 177 (2022) 106092

Contents lists available at ScienceDirect

Pharmacological Research

journal homepage: www.elsevier.com/locate/yphrs

Kinsenoside attenuates liver fibro-inflammation by suppressing dendritic cells via the PI3K-AKT-FoxO1 pathway

Ming Xiang [a,1], Tingting Liu [b,1], Cheng Tian [a,1], Kun Ma [a], Jing Gou [a], Rongrong Huang [c], Senlin Li [a], Qing Li [a], Chuanrui Xu [a], Lei Li [a], Chih-Hao Lee [d], Yonghui Zhang [e,*]

[a] Department of Pharmacology, School of Pharmacy, Tongji Medical College, Huazhong University of Science and Technology, Wuhan, Hubei, China
[b] Department of Pharmacy, the First Affiliated Hospital of Anhui Medical University, the Grade 3 Pharmaceutical Chemistry Laboratory of State Administration of Traditional Chinese Medicine, Hefei, Anhui, China
[c] Department of Pharmacy, Union Hospital, Tongji Medical College, Huazhong University of Science and Technology, Wuhan, Hubei, China
[d] Department of Genetics and Complex Diseases, Harvard School of Public Health, Boston, MA, USA
[e] Hubei Key Laboratory of Natural Medicinal Chemistry and Resource Evaluation, School of Pharmacy, Tongji Medical College, Huazhong University of Science and Technology, Wuhan, Hubei, China

ARTICLE INFO

Keywords:
Liver fibro-inflammation
Kinsenoside
Dendritic cell
PI3K-AKT-FoxO1 axis
Programmed cell death ligand 1
Interleukin-12

Chemical compounds studied in this article:
Kinsenoside (PubChem CID:10422896)
LY294002 (PubChem CID:3973)
740 Y-P (PubChem CID:90488730)

ABSTRACT

Kinsenoside (KD) exhibits anti-inflammatory and immunosuppressive effects. Dendritic cells (DCs) are critical regulators of the pathologic inflammatory milieu in liver fibrosis (LF). Herein, we explored whether and how KD repressed development of LF via DC regulation and verified the pathway involved in the process. Given our analysis, both KD and adoptive transfer of KD-conditioned DCs conspicuously reduced hepatic histopathological damage, proinflammatory cytokine release and extracellular matrix deposition in CCl_4-induced LF mice. Of note, KD restrained the LF-driven rise in CD86, MHC-II, and CCR7 levels and, simultaneously, upregulated PD-L1 expression on DCs specifically, which blocked $CD8^+$T cell activation. Additionally, KD reduced DC glycolysis, maintained DCs immature, accompanied by IL-12 decrease in DCs. Inhibiting DC function by KD disturbed the communication of DCs and HSCs with the expression or secretion of α-SMA and Col-I declined in the liver. Mechanistically, KD suppressed the phosphorylation of PI3K-AKT driven by LF or PI3K agonist, followed by enhanced nuclear transport of FoxO1 and upregulated interaction of FoxO1 with the PD-L1 promoter in DCs. PI3K inhibitor or si-IL-12 acting on DC could relieve LF, HSC activation and diminish the effect of KD. In conclusion, KD suppressed DC maturation with promoted PD-L1 expression via PI3K-AKT-FoxO1 and decreased IL-12 secretion, which blocked activation of $CD8^+$T cells and HSCs, thereby alleviating liver injury and fibro-inflammation in LF.

1. Introduction

Liver fibrosis (LF)[2] is a chronic condition with multifactorial pathology, and it poses a significant risk of progression into hepatocellular carcinoma[1]. In LF, hepatic immunity is altered and liver inflammation occurs, ultimately resulting in hepatic stellate cell (HSC)[3] activation, extracellular matrix (ECM) deposition and fibro-inflammation[2]. The animal treated with carbon tetrachloride (CCl_4) is the classic LF model. In the early stage of CCl_4-induced LF, free radical compound (CCl_3 and Cl) in liver damages hepatocytes[3]. Then, injured hepatocytes disrupt immune homeostasis, and stimulate aberrant immune cell activity[4]. After being activated by damaged hepatocytes, innate immune cells, especially dendritic cells (DCs), recruit and activate $CD8^+$T effector cell [5]. $CD8^+$T cells in turn aggravate hepatocyte injury by releasing

Abbreviations: AKT, protein kinase B; BMDC, bone marrow-derived debdritic cell; DC, dendritic cell; ECM, extracellular matrix; FoxO1, forkhead box protein O1; HSC, hepatic stellate cell; IL-12, interleukin-12; KD, kinsenoside; LF, liver fibrosis; LPS, lipopolysaccharide; MFB, myofibroblast; PD-L1, programmed cell death ligand 1; PI3K, phosphatidylinositol 3 kinase.

* Corresponding author.
E-mail address: zhangyh@tjmu.edu.cn (Y. Zhang).

[1] These authors contributed equally to this work.
[2] LF: liver fibrosis
[3] HSC: hepatic stellate cell

https://doi.org/10.1016/j.phrs.2022.106092
Received 1 September 2021; Received in revised form 16 January 2022; Accepted 18 January 2022
Available online 21 January 2022

cytotoxic cytokines[6]. The secondary attack of immune cells results in the aggravation of hepatocyte injury and fibro-inflammation[7]. In addition, injured hepatocytes and activated immune cells transformed quiescent HSCs, the most important cell involved in LF, to myofibroblasts (MFB) via cell cross-talk[8].

DCs are critical for the regulation of liver immunity, and irregular DC activity can induce the activation of T cells and HSCs to contribute to the pathological inflammation-rich environment and fibrogenesis [9]. The immaturation and immunosuppression of DCs could be mediated by programmed cell death ligand 1 (PD-L1), the ligand of programmed cell death 1 (PD-1)[10]. Immunosuppressed DCs produced fewer pro-inflammatory cytokines, such as IL-12. The IL-12 heterodimer containing IL-12 *p40* and IL-12 *p35* was reported to be correlated with LF and HSC activation[11]. Therefore, inducing DC immunosuppression may be an attractive approach to experimental therapeutics in liver fibro-inflammatory disease. Recently, DC function was reported to be associated with the phosphatidylinositol 3 kinase/protein kinase B (PI3K-AKT) axis, which was implicated in reprogramming immune cell functions, controlling cellular responses (survival, proliferation, and metabolism), and regulating LF[12,13]. The PI3K-AKT axis was activated in DCs stimulated by lipopolysaccharide (LPS), and LY294002 (PI3K inhibitor) blocked the activation of DCs[14]. One mechanism of PI3K-AKT-mediated regulation of cellular function involves the phosphorylated inactivation of the forkhead box protein O1 (FoxO1)[15]. Being a transcription factor, FoxO1 is capable of binding to gene promoters in the nucleus and regulating expression of target genes. However, the AKT-mediated phosphorylation of FoxO1 causes FoxO1 exit from the nucleus, along with the suppression of FoxO1 activity[16]. Multiple studies have highlighted FoxO1 involvement in LF progression, along with the maturity and function of DCs[17,18].

Anoectochilus roxburghii (*A. roxburghii*), widespread in tropical regions, is a traditional herb native to China[19]. Kinsenoside (KD[4] 3-(R)− 3-β-D-Glucopyranosyloxybutanolide) is a biologically active component of *A. roxburghii* (Fig. S1A). Emerging evidences revealed a wide array of pharmacological benefits of KD, including anti-hyperglycemia, anti-hyperlipidemia, anti-osteoarthritis, renoprotection and immunosuppression[20–23]. Besides, KD ameliorated oxidative damage against retinal pigment epithelium and subsequent angiogenesis via ERK/p38/NF-κB pathway[24], and protected advanced glycation end products (AGEs)-induced endothelial dysfunction through AGEs-RAGE-NF-κB pathway[25]. A prior study demonstrated that KD exerted a hepato-protective effect on CCl_4-induced LF mice and in patients with liver disease, but the mechanism is currently unknown[26].

Given these evidences, KD is possible to ease LF via enhancing DC immunosuppression. To further explore this, we detected the role of KD in LF therapy and mechanism in vivo, *in vitro* and applying cell adoptive transfer model. The results suggested that KD exhibited attenuated effects on fibro-inflammation and LF by inhibiting DC maturation and function, which was attributed to promoting FoxO1 binding to PD-L1 promoter in DCs via PI3K-AKT-FoxO1 axis.

2. Materials and methods

2.1. Animals and ethical approval

Male 6-week-old C57BL/6J mice, with body weight between 18 and 22 g, were procured from the Beijing Vital River Laboratory Animal Technology Co. Ltd (Beijing, China) and housed in cages (6 mice/cage) at the Experimental Animal Center of Tongji Medical College (Huazhong University of Science and Technology, Wuhan, China) under strict pathogen free environment. The temperature was set to 25 ℃, with a regular 12:12 h (light/dark) cycle and the mice were provided with standard laboratory diet and tap water throughout the experiments. Our protocols followed the 3Rs (replacement, refinement, reduction). Mice assessment was carried out by an investigator who was blinded to the grouping of mice. Animal care and experimental procedures were carried out in accordance with the guidelines of the Tongji Medical College, Huazhong University of Science and Technology Institutional Animal Care and Use Committee (IACUC Number: 2505).

2.2. Preparation of KD

A. roxburghii was extracted by immersion in water four times at 80 ℃ until the crude of ethanol reached 95%. The supernatant was obtained and subjected to a silica gel chromatography column elution with chloroform-ethanol (4:1). The eluents with KD were combined under the direction of thin layer chromatography to produce a crude KD sample, which was further washed with ethanol to obtain pure KD. The purity of KD (>98%) was analyzed using a high-pressured liquid chromatography with an evaporative light scattering detector (Fig. S1B), and identification was done with nuclear magnetic resonance (NMR), based on data from a prior report[27].

2.3. CCl_4-induced fibro-inflammation models and KD therapy

As reported previously, 6-week-old C57BL/6J mice received intraperitoneal injection of 10% CCl_4 (dosage: 2 mL/kg) two times a week for 8 weeks to induce LF[28]. Mice were treated by oral gavage with KD (30, 20, 10 mg/kg) or solvent (saline) once a day for 8 weeks. The dose of KD was determined by our concentration screening tests. KD effect on alanine aminotransferase (ALT) and aspartate aminotransferase (AST) levels in the serum of CCl_4-treated mice showed the visible dose-effect relationship from 10 to 30 mg/kg. KD (30 mg/kg) treatment in the absence of CCl_4 was used to investigate the toxicity of KD to healthy mice. Silymarin (50 mg/kg), which was used in clinical settings against LF, served as positive drug. Mice were anesthetized with tribromoethanol (400 mg/kg, ip.) before the experiment.

2.4. Cell culture and KD treatment

DCs and T lymphocytes were prepared as described before[29]. (1) Bone marrow-derived DCs (BMDCs, $CD11c^+$) were isolated from bone marrow and cultured in RPMI 1640 medium (HyClone, Beijing, China) with cytokines granulocyte macrophage colony stimulating factor (GM-CSF) (20 μg/mL, Peprotech, Rocky Hill, NJ, USA) and interleukin-4 (IL-4) (10 ng/mL, Shanghai ExCell Biology Inc. Shanghai, China) for 7 days. DC maturity was induced with LPS (10 μg/mL) for 24 h and flow-cytometrically identified with $CD11c^+$. (2) $CD8^+$T cells were extracted and isolated from spleen using a $CD8a^+$T cell isolation kit (MACS, Miltenyi Biotec Inc. Auburn, CA, USA), and were activated with concanavalin A (ConA, 5 μg/mL) for 24 h. (3) Murine hepatic stellate cells (JS-1) were acquired from the Shanghai Yaji Biological Co. LTD, China, and grown in DMEM/F-12 medium (HyClone, Beijing, China) with 10% fetal bovine serum. JS-1 was activated with TGF-β_1 (5 ng/mL, Peprotech) for 24 h[30]. Cells were incubated with KD (10, 5, and 2.5 μg/mL, dissolved by phosphorylated buffer solution), as determined by concentration screening tests for 24 h (effect of KD on the mixed lymphocyte reaction and cytokine secretion of DCs in vitro showed the obvious dose-effect relationship from 2.5 to 10 μg/mL). All cells were maintained at 37 ℃ in an incubator with 5% CO_2. The cells were treated with agonists to simulate inflammation or injury microenvironment reflecting the in vivo conditions.

2.5. Adoptive transfer KD-conditioned DCs to LF mice

BMDCs were exposed to LPS (10 μg/mL, 24 h) to harvest the LPS-treated mature BMDCs, and treated with LPS and KD (5 μg/mL, 24 h) to obtain the KD-conditioned BMDCs. Subsequently, the mice were transplanted with different BMDCs (5 $\times 10^6$ cells each mouse), as

[4] KD: kinsenoside

CCl_4+DC, and CCl_4+KD-conditioned DC respectively, via tail vein injection on day-1, day-8, and day-15 after 6 week-CCl_4 exposure[31]. Controls and CCl_4 mice were injected with equal volume of phosphate buffered saline. The LF status was then analyzed pathologically, immunologically, and serologically.

Meanwhile, the biodistribution of injected DCs was tested by DiR-labeled[32]. In detail, BMDCs were suspended in 5 μg/mL DiR buffer and incubated at 37 ℃ for 20 min to produce DiR-labeled DCs. Afterward, the DiR-labeled DCs were administered to mice via tail vein injection. Liver, spleen, kidney, lung and heart were obtained and imaged by Pear Trilogy System (Odyssey CLX, LI-COR, NE, USA) on day-1, day-3, day-5, day-7. A technical route of the animal experiment design was showed in Fig. S1C.

2.6. Cross interaction assay of DCs and JS-1

To characterize the KD-mediated regulation of JS-1 cross-priming response to DCs *ex vivo*, approximately 3×10^4 BMDCs were co-cultured with 3×10^5 JS-1 in a transwell with RPMI 1640 medium for 24 h. BMDCs from normal or LF mice were plated in the apical chamber surface of the bottom membrane of transwell-24 well inserts (Costar, Corning Inc., USA) in the presence or absence of KD, si-IL-12, or KD+si-IL-12 for 12 h. Then, the supernatant was discarded and the transwell was transferred to a new well containing 3×10^5 JS-1 with or without IL-12 supplement in the lower layer for 48 h[33]. Subsequently, the activation and ECM secretion of JS-1 were assessed via quantitative real-time-PCR (qPCR), western blot, and immunofluorescence (IF).

2.7. Hepatocyte injury and cell apoptosis assay

AML-12 (mouse hepatocyte) was treated with 400 mmol/L alcohol for 24 h or 20 mmol/L CCl_4 for 48 h to produce the hepatocyte injury model[33,34]. Cell apoptosis was examined with a FITC-Annexin V Apoptosis Detection Kit (BD Biosciences, Franklin, NJ, USA), as per operational guidelines. Upon 24 h or 48 h treatment, the cells were exposed to EDTA-free trypsin and re-suspended in 1 ×binding buffer, before exposure to FITC-Annexin V and PI at room temperature (RT) for 15 min. Finally, the apoptotic rate was assessed via FCM.

2.8. Histological, immunohistological and IF studies

Liver sections underwent staining with hematoxylin and eosin (H&E) and sirius red for histopathological examination. Immunohistochemical staining was carried out with α-smooth muscle actin (α-SMA)-specific polyclonal antibody (Proteintech, Wuhan, China). IF was conducted on JS-1 and DCs using anti-α-SMA (Proteintech) and anti-FoxO1 (Cell Signaling Technology, Danvers, MA, USA) antibodies, respectively, with subsequent exposure to Alexa Fluor 594 donkey anti-rabbit IgG (Antgene, Wuhan, Hubei, China).

2.9. Flow cytometry (FCM) analysis

Immune cells from the liver and bone marrow were analyzed by FCM. Briefly, the cells underwent staining with fluorochrome-antibodies (eBioscience, California, USA and BD Biosciences, Franklin, NJ, USA) targeting cell surface antigens at 4 ℃ for 60 min (1) DCs were stained with the FITC-CD11c, APC-CD86, and PE-major histocompatibility complex II (MHC-II). $CD11c^+$ cells were screened out from live cells and the expressions of MHC-II and CD86 were calculated in $CD11c^+$ cell gate. The gate was chosen by the compare between negative cells (without fluorescent dye) and single fluorescent dye cells. PD-L1 or CCR7 positive DCs were identified with PE-CD274 or APC-CCR7, respectively, from $CD11c^+$ cell gate. (2) $CD8^+$T cells were stained with APC-CD3 and PE-CD8 and $CD4^+$T cells with APC-CD3 and FITC-CD4. (3) Natural killer T (NKT) cells and NK cells were stained with APC-CD3 and PE-NK1.1. (4) Myeloid-derived immunosuppressive cells (MDSCs) received staining with APC-CD11b and PE-Gr1. (5) Macrophages in liver were stained with FITC-CD11b and PE-F4/80. Moreover, M1-type or M2-type macrophage in vivo was identified with APC-CD86 or Alexa 647-CD206, respectively. M1-type or M2-type of RAW264.7 in vitro was identified with FITC-CD86 or Alexa 647-CD206, respectively.

2.10. siRNA and plasmid transfection

FoxO1 and negative siRNAs were acquired from the Viewsolid Biotech (Beijing, China). The following list belongs to the target sequences of these siRNAs: *siFoxO1-mus-1362* (5′ - GCA ACG AUG ACU UUG AUA ATT - 3′, 5′ - UUA UCA AAG UCA UCG UUG CTT - 3′), *siFoxO1-mus-1532* (5′ - CCC AGU CUG UCU GAA AUC ATT - 3′, 5′ - UGA UUU CAG ACA GAC UGG GTT - 3′), *siFoxO1-mus-1083* (5′ - GAG GAU UGA ACC AGU AUA ATT - 3′, 5′ - UUA UAC UGG UUC AAU CCU CTT - 3′), and *negative control* (5′ - UUC UCC GAA CGU GUC ACG UTT - 3′, 5′ - AGC UGA CAC GUU CGG AGA ATT - 3′). All cells in this study were transfected with the siRNA using the GenMute™ siRNA Transfection Reagent (SignaGen Laboratories), following operational guidelines. The siFoxO1-mus-1362-transfected cells exhibited optimal interference efficiencies (Data not shown). We, therefore, selected siFoxO1-mus-1362 for use in our experiment, and its interference effect is presented in Fig. S1D. The siRNA sequences specific for *IL-12 p40* (5′ - GAU GAC AUC ACCUGGACCUTT - 3′,5′ - AAG AUG ACA UCA CCU GGA CCU - 3′) and negative control (5′ - UUC UCC GAA CGU GUC ACG UTT - 3′, 5′ - ACG UGA CACGUU CGG AGAATT - 3′) was chosen, based on the Hill et al. study and synthesized by GenePharma (Suzhou, China)[35] (Fig. S1E).

2.11. Chromatin immunoprecipitation (ChIP) assays

ChIP assays were done with Simple ChIP Plus Enzymatic Chromatin IP Kit (Agarose Beads). In brief, 1% formaldehyde was used to fix the cells before the DNA was nicked with enzymes and immunoprecipitated with anti-FoxO1 or matched control antibody, prior to capture with magnetic protein G beads. The ChIP DNA was then real-time PCR-amplified with SYBR green and primers against *PD-L1* (5′ - GCT AAT GCA GGT TTC ACT TTC AC - 3′, 5′ - GCA GGT GAG TCT CTG GTC TAT - 3′).

2.12. Enzyme-linked immunosorbent assay (ELISA), NO release, and glucose uptake test

Levels of ALT, AST, IL-2, IL-10, interferon-γ (IFN-γ), total IL-12, and tumor necrosis factor-α (TNF-α) in serum or cell culture supernatant were assessed with the ELISA assay (eBioscience, San Diego, CA, USA). Levels of TGF-β_1, matrix metalloproteinase (MMP)− 13, tissue inhibitor of metalloproteinase (TIMP)− 1, TIMP-2, and collagen-I (Col-I) in liver homogenate or cell culture supernatant were assessed with the ELISA assay (Ruixin Biotech, Quanzhou, China). NO production in serum was quantified by griess reagent (Beyotime, Shanghai, China). Glucose uptake was examined with the glucose oxidase-peroxidase technique, using a glucose test kit (Rsbio, Shanghai, China).

2.13. Glycolysis and respiration of DCs

The cells were incubated in a 24-well Agilent Seahorse XF Cell Culture Microplate (Agilent Technologies, Inc., Santa Clara, CA, USA), at 10^4 cells per well. Next, the plate was placed in a 37 ℃ incubator to allow for cell adherence. Subsequently, the culture medium was removed and specific medium from the kit was introduced to the cells, which were then incubated without CO_2. Detecting drugs were introduced to the cells, according to kit instructions. For oxygen consumption, the drugs used were oligomycin, carbonyl cyanide-4-trifluoromethoxyphenylhydrazone (FCCP), rotenone, and antimycin A. In addition, for the glycolysis stress test, we used glucose, oligomycin, and 2-Deoxy-D-glucose (2-DG).

2.14. Mixed lymphocyte reaction (MLR) and cell proliferation assay

BMDCs extracted from control, LF, and LF mice exposed to KD (30 mg/kg) were cultured as mentioned before. Spleen $CD8^+$T cells from normal mice and DCs subjected to different treatments were co-cultured at ratios of 10:2 and 10:1 for 48 h[36]. $CD8^+$T cell proliferation was examined with cell counting kit-8 (CCK8) assays at 450 nm using a multi-well plate reader.

2.15. Western blot

Protein extracts were separated on 10% SDS-polyacrylamide gels, followed by electro-blotting transfer to polyvinylidenedifluoride (PVDF) membranes. Blocking was done for 1 h at RT, before overnight incubation in various primary antibodies at 4 ℃. The specific primary antibodies used in this study were PI3K, p-PI3K (Tyr458), AKT, p-AKT (Ser473), FoxO1 (Cell Signaling Technology, Danvers, MA, USA), p-FoxO1 (Ser256) (Signalway Antibody, College Park, MA, USA), α-SMA (Proteintech), GAPDH (Bioswamp, Wuhan, China), and Histone 3 (Sungene Biotech, Shanghai, China). Next, the membranes were exposed to the subsequent secondary antibodies (1:10000) at RT for 1 h, before detection with an ECL chemiluminescence detection kit (Amersham Biosciences UK Ltd., Buckinghamshire, UK) or Double IR Laser Imager (Odyssey CLX, LI-COR, NE, USA). Normalization was done based on the level of GAPDH or Histone 3 in samples.

2.16. Quantitative real-time-PCR (qPCR)

Total RNA was isolated from liver tissues, DCs, and JS-1 with TRIzol, as per kit directions, and used as templates to form cDNA using the transcription kit (Promega, Madison, WI, USA). Subsequently, the cDNA was amplified via incubation at 95 ℃ for 5 min, with a thermal cycle profile of 40 cycles of denaturation at 95 ℃ for 10 s, annealing at 55–60 ℃ for 20 s, and extension at 72 ℃ for 30 s. Normalization of relative gene expression was done with levels of endogenous GAPDH. The corresponding gene primer sequences are summarized in Table S1.

2.17. Statistical analysis

SPSS 16.0 software program (SPSS Software Products, Chicago, IL, USA) was employed for all statistical analyses. Data are expressed as mean ± SD. Multi-group comparisons were conducted via one-way analysis of variance (ANOVA), whereas inter-group comparisons were done with the Dunnett's *t* test. $P < 0.05$ denoted significance. Some data were normalized to avoid unwanted sources of variation. Data from all experiments were collected and evaluated in a blinded manner.

3. Results

3.1. KD exerted liver-protective and anti-inflammatory effects on CCl_4-induced LF

In CCl_4-induced LF mice, oral administration of 30, 20, or 10 mg/kg KD markedly diminished the extent of LF with substantial lymphocyte infiltration and collagen deposition (Fig. 1 A). In line with the macroscopic changes, the serum ALT and AST levels, along with the liver index conspicuously decreased with KD treatment (Fig. 1B). Furthermore, KD lowered the production of pro-inflammatory cytokines like IL-2, IFN-γ, TNF-α, and IL-12, and raised the secretion of anti-inflammatory cytokines IL-10. KD also reduced NO release, thus, lowering inflammatory responses (Fig. 1 C and D). In addition, KD suppressed expression or release of fibrosis-related proteins, including α-SMA, TGF-β_1, Col-I, and TIMP-1 and TIMP-2, but augmented the mRNA and protein level of MMP-13, thus degrading the ECM (Fig. 1 A, E and F). The results demonstrated that KD exerted liver-protective, anti-inflammatory and anti-fibrotic effects on CCl_4-induced LF.

Interestingly, the effects of KD were comparable to or better than those of silymarin, which was used in clinical settings against LF. In addition, KD had no effect on the serum ALT, AST levels or on the fibro-inflammatory histopathological damage and fibrosis agents in healthy mice (Fig. S2A and B). In additional, KD had no adverse effect on heart, lung, spleen, and kidney in healthy mice (Fig. S2C), and did not alter the survival rate of normal hepatocyte AML-12 (Fig. S2D). These data suggested that KD strongly suppressed fibro-inflammation in LF, without causing any serious adverse reactions.

3.2. Indirect effects of KD on $CD8^+$T cells and HSCs

Numerous immune cells regulate the development of hepatic fibro-inflammation[37]. We quantitatively determined the proportions of various hepatic immune cells, involved in the CCl_4-driven LF. After CCl_4 administration, DC maturity and $CD8^+$T cell differentiation were greatly enhanced, and M2-type macrophage polarization reduced slightly in the liver. KD reversed the CCl_4-mediated regulation of DCs, $CD8^+$T cells, and M2-type macrophages, and had little effect on other subtypes of immune cells in the liver (Fig. S3).

Of note, in vitro, KD also strongly retarded BMDC maturation and function (Fig. S4A-C). However, KD repolarized M1 macrophages to the M2 phenotype marginally (Fig. S4D). And there was no obvious regulation of KD to magnetic bead sorting spleen $CD8^+$T cell proliferation (Fig. S4E). The different effect of KD on $CD8^+$T cells in vivo and in vitro suggested that KD effect on $CD8^+$T cells might be indirect.

Given the vital role of hepatocyte injury and HSC activation in LF and to identify potential target cells of KD, the effect of KD on JS-1 (mouse HSCs) and AML-12 (mouse hepatocytes) were further examined in vitro. Only high dose of KD lowered the expression and secretion of Col-I, TIMP-1, and TIMP-2, but did not alter the levels of α-SMA, as well as the apoptotic status of JS-1, compared to TGF-β_1 group (Fig. 2). In contrast to its predominant effect in vivo, KD exhibited a poor effect on HSCs in vitro. Additionally, CCl_4 or alcohol induced apoptosis and ALT and AST release from AML-12, but KD did not relieve the injury of AML-12 directly (Fig. S5). The apparent modulation loop involving interactions of DCs and $CD8^+$T cells might be important to maintain immune homeostasis during progression of LF.

3.3. KD repressed DC responses in LF mice

In vivo, we observed that KD reduced the levels of MHC-II and co-stimulator CD86 on $CD11c^+$ BMDCs (Fig. 3 A). It inhibited CCR7, but substantially elevated levels of the negative regulatory molecule PD-L1 on $CD11c^+$ BMDCs (Fig. 3B and C). The level of indoleamine-2,3-dioxygenase (*IDO*), a tolerant DC-secreted anti-inflammatory agent, was also elevated upon KD exposure (Fig. 3 C). Moreover, KD down-regulated levels of IL-12, an essential DC-secreted inflammatory agent (Fig. 3 C and D). In addition, using MLR, we revealed that KD significantly downregulated the DC-mediated induction of $CD8^+$T lymphocyte proliferation *ex vivo* (Fig. 3E).

Following maturity, DC metabolism shift toward glycolysis[38]. We analyzed DC glucose metabolism after KD treatment. The results demonstrated that KD suppressed glucose utilization, *Glut1* expression, glucose uptake, and glycolysis-related genes expressions in BMDCs. Additionally, oxygen consumption and ATP generation were weakened in BMDCs after KD treatment (Fig. S6). Since the maturation of DCs mainly depends on increased ATP flux via the glycolytic pathway[38], it seems reasonable to consider that KD exerts its immunosuppressive effects in DCs at least in part by suppressing glycolysis in DCs. Immunogenic DCs serve a critical role in antigen presentation during early immune response. In all, these data suggest that the KD-mediated immunosuppressive and anti-inflammatory properties may largely ascribe to the suppression of DC maturation and function in LF.

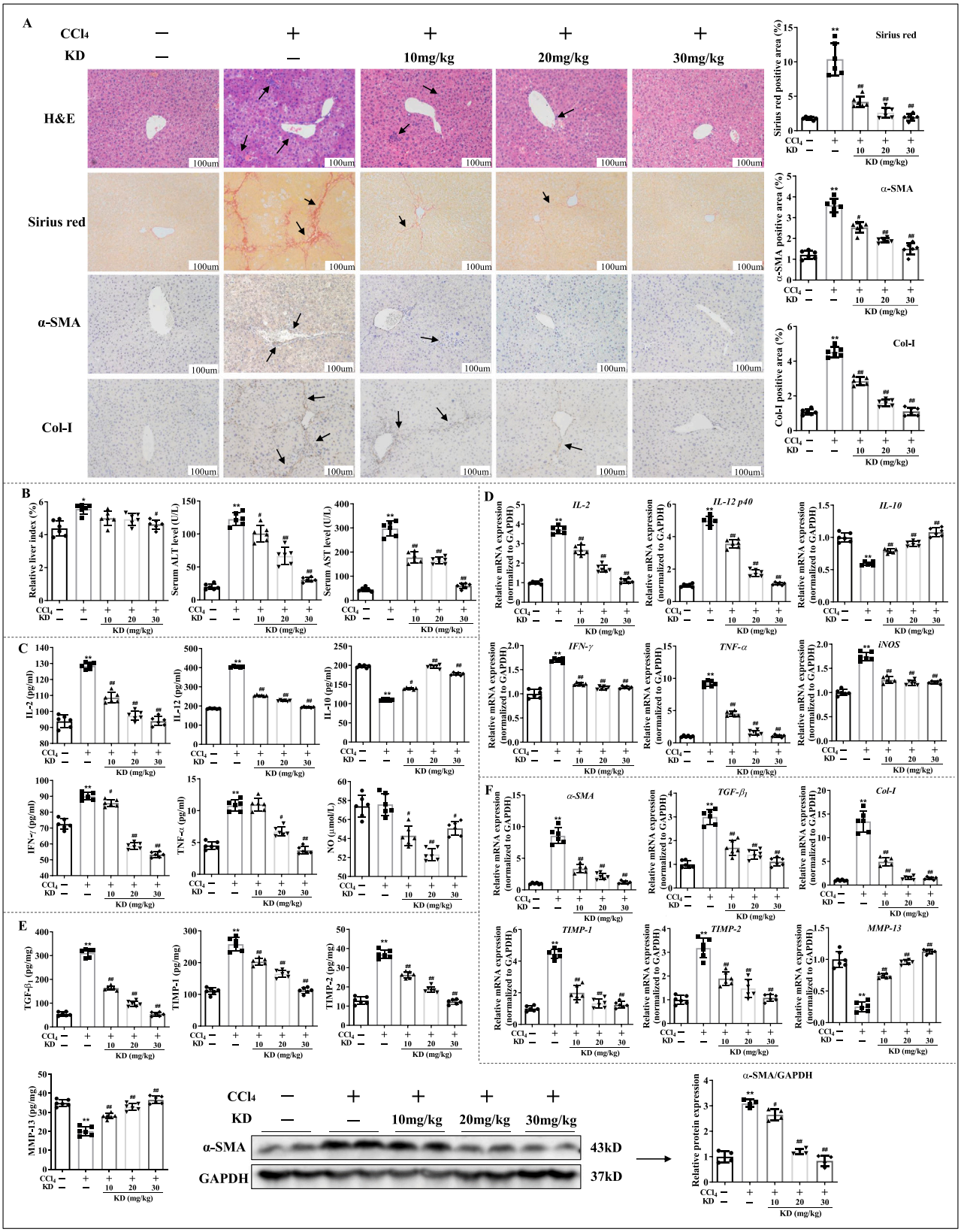

Fig. 1. KD abolished hepatic fibro-inflammation in CCl_4 mice. (A) Representative images of H&E (arrows represent inflammatory infiltrations), sirius red (arrows indicate collagenous fiber deposition), and α-SMA immunohistochmical antibody (arrows represent α-SMA expression) or Col-I immunohistochmical antibody (arrows represent Col-I expression) stained liver sections. Original magnification, 200 × ; scale bar, 100 μm. (B) Levels of ALT and AST in serum, and liver index (liver wet weight/mouse body weight×100%). (C) Serum inflammatory cytokine concentrations. (D) Transcript levels of hepatic inflammatory cytokines. (E) Content of TGF-β_1, TIMP-1, TIMP-2, and MMP-13 in liver homogenate and levels of hepatic α-SMA protein. (F) Hepatic mRNA levels of *α-SMA*, *TGF-β_1*, *Col-I*, *TIMP-1*, *TIMP-2*, and *MMP-13*. Data expressed as mean ± SD (n = 6). $^{*}P < 0.05$, $^{**}P < 0.01$ relative to controls; $^{\#}P < 0.05$, $^{\#\#}P < 0.01$ relative to CCl_4-induced LF mice.

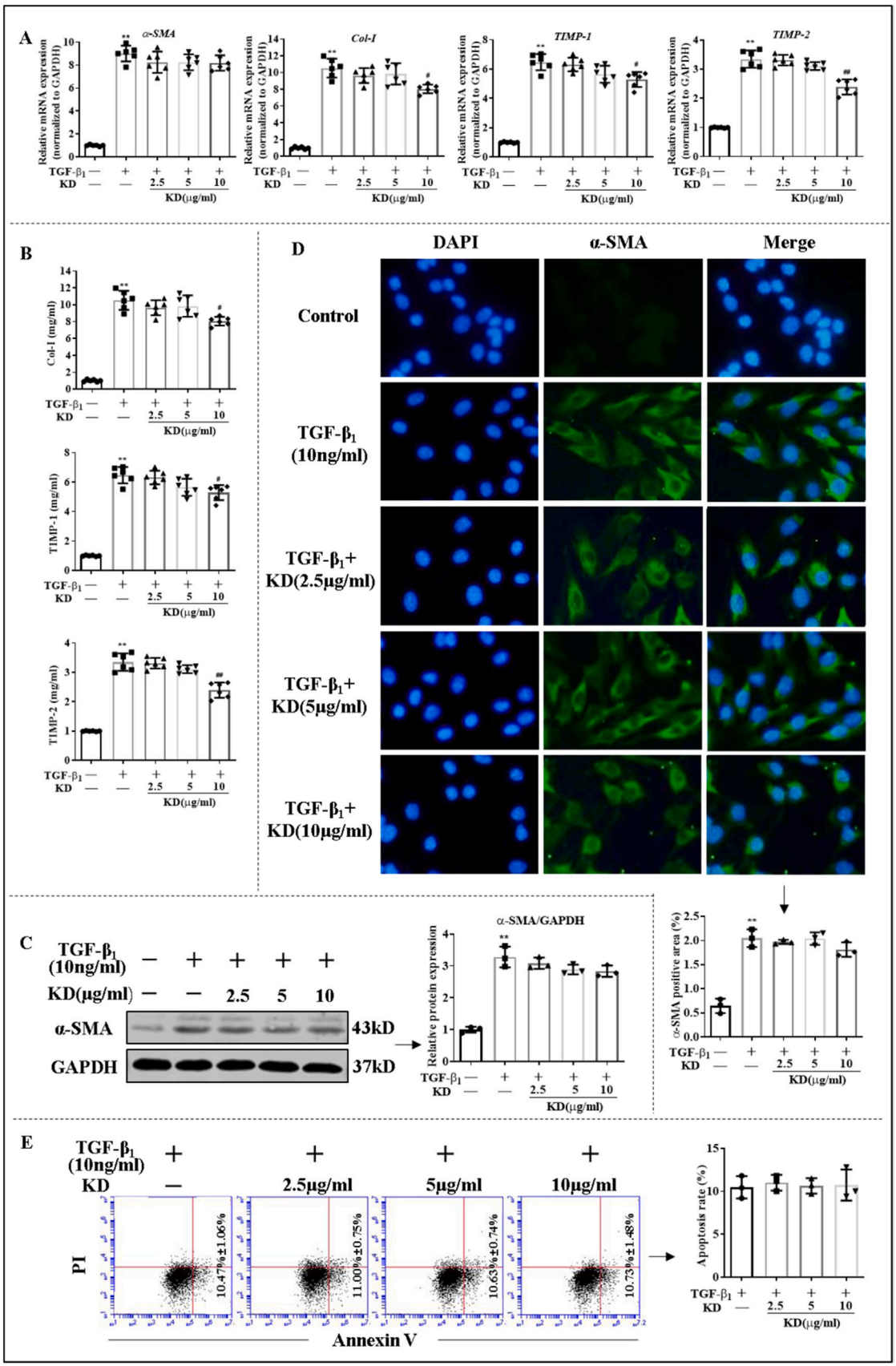

Fig. 2. The effects of KD on HSCs (JS-1) in vitro. (A) The mRNA levels of *α-SMA*, *Col-I*, *TIMP-1*, and *TIMP-2* in JS-1. (B) Extracellular release levels of Col-I, TIMP-1, and TIMP-2 in JS-1. (C) Levels of α-SMA protein in JS-1. (D) Immunofluorescence of α-SMA protein in JS-1. (E) Apoptotic rate of JS-1. Data expressed as mean ± SD (n = 6). $^{**}P < 0.01$ relative to controls; $^{\#}P < 0.05$, $^{\#\#}P < 0.01$ relative to TGF-β_1 group.

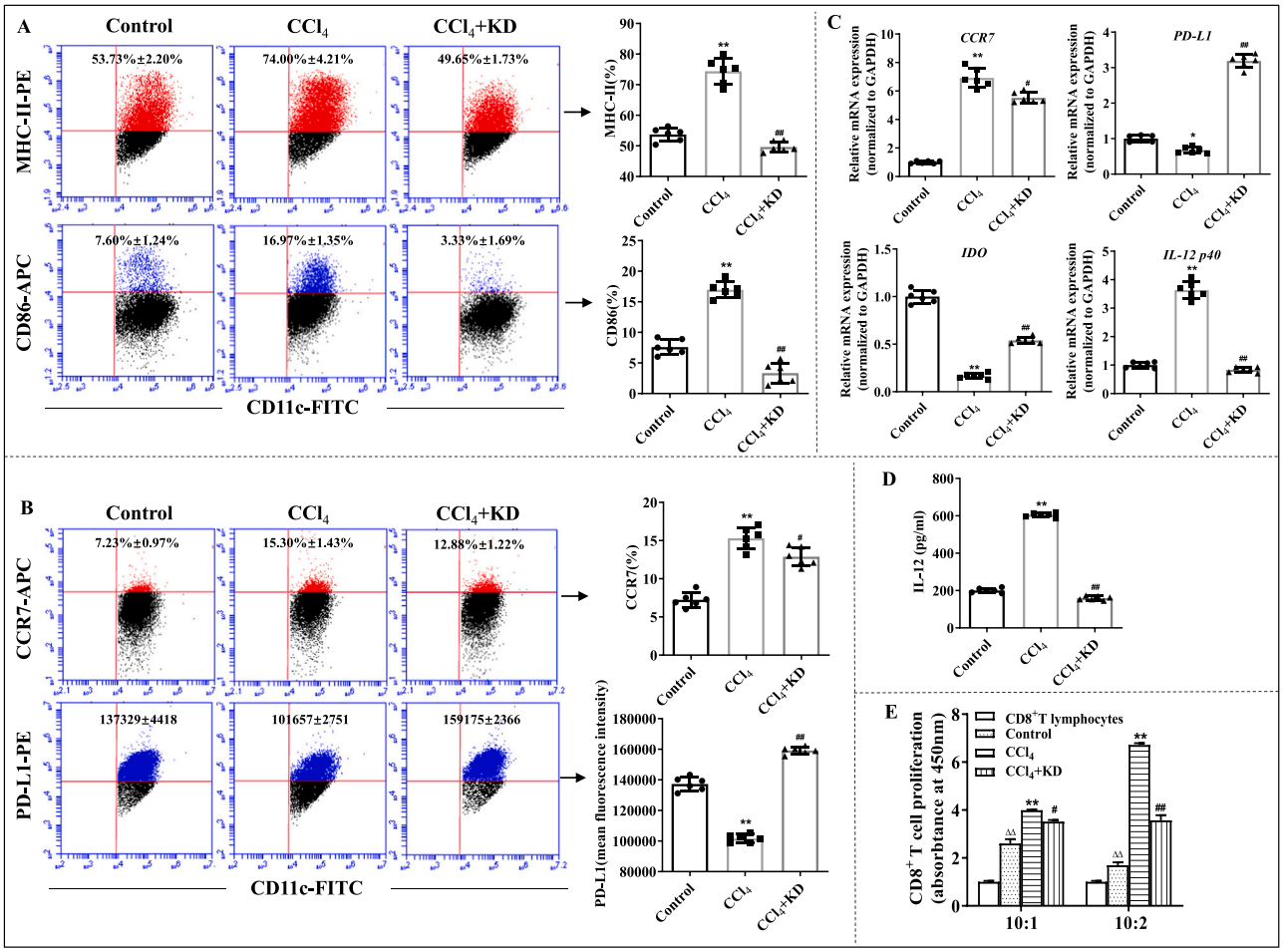

Fig. 3. KD inhibited the maturity and function of BMDCs *ex vivo*. (A) The percentage of MHC-II$^+$ cells and CD86$^+$ cells on CD11c$^+$ BMDCs. (B) The percentage of CCR7 and mean fluorescence intensity of PD-L1 on CD11c$^+$ BMDCs, as evidenced by FCM. (C) Gene levels of *CCR7*, *PD-L1*, *IDO*, and *IL-12 p40*, as quantified by qPCR. (D) Amount of IL-12 release in DC suspension, as analyzed by ELISA. (E) The DC-mediated induction of CD8$^+$T cell proliferation, as evaluated by MLR. The ratio of CD8$^+$T cells and DCs was 10:2 and 10:1. BMDCs were isolated from controls, CCl_4-induced LF mice, and LF mice exposed to KD (30 mg/kg). Data expressed as mean ± SD (n = 6). $^*P < 0.05$, $^{**}P < 0.01$ relative to controls; $^{\#}P < 0.05$, $^{\#\#}P < 0.01$ relative to CCl_4 group; $^{\Delta\Delta}P < 0.01$ relative to the CD8$^+$T lymphocytes group, which is in the absence of DC stimulation.

3.4. Adopting KD-conditioned DCs ameliorated LF, inflammation, and inhibited CD8$^+$T cell differentiation

To determine the immunomodulatory effect of KD-conditioned DCs on experimental LF and CD8$^+$T cells, LF mice were injected with KD (5 μg/mL)-treated DCs via tail vein. To estimate the distribution of injected DCs, DiR-labeled DCs were administrated to mice in the same way, and high Dir fluorescence was found in the liver of mice (Fig. S7). The results demonstrated that adoptive transfer DCs was abundant in the liver and adoptive transfer of KD-conditioned DCs to LF mice diminished the severity of fibro-inflammation in the liver. The expression of α-SMA, a HSC activation-related gene, in the liver was also been suppressed by KD-conditioned DCs (Fig. 4 A and B). Moreover, we also observed alterations in the gene expression: *α-SMA*, *TGF-β_1*, *Col-I*, and *TIMP-1/− 2* levels were reduced, whereas *MMP-13* levels were elevated (Fig. 4 C). Additionally, in mice treated with KD-conditioned DCs, pro-inflammatory cytokines were diminished and anti-inflammatory cytokines were elevated in both serum and liver (Fig. 4D and E). Hepatic CD8$^+$T cell levels were low in the LF mice with KD-conditioned DCs versus LF models (Fig. 4 F). Collectively, these results indicate that KD-conditioned DCs disrupts HSC and CD8$^+$T cell responses, and that DCs are indispensable to the action of KD on LF.

3.5. KD resulted in immature phenotype and insufficient function of DCs, mediated by the PI3K-AKT-FoxO1 axis

In our previous study, the PI3K-AKT axis was found to contribute to KD effect on autoimmune hepatitis[39]. Here, we revealed that KD strongly suppressed phosphorylation of PI3K (Tyr458) and AKT (Ser473), without affecting their mRNA and total protein expressions in BMDCs isolated from LF mice (Fig. 5 A and B). The total protein and phosphorylation of FoxO1 (Ser256) were increased in BMDCs from LF mice compared with controls, which contributed to FoxO1 exit from the nucleus. KD decreased the FoxO1 in the cytoplasm by reducing FoxO1 phosphorylation in BMDCs (Fig. 5A-E).

Following the 740 Y-P (20 μg/mL, 24 h)-mediated activation of PI3K, DCs exhibited a mature phenotype, with enhanced levels of MHC-II, CD86, and CCR7, elevated secretion of IL-12, and lowered expression of PD-L1 and *IDO*. KD, on the other hand, eliminated the impact induced by 740 Y-P pre-treatment (Fig. S8A-C). Meanwhile, we pre-treated LPS-induced DCs with LY294002 (PI3K inhibitor), which retarded maturity and function of DCs. Adding KD did not enhance the effect of LY294002, which suggested that the main signal target of KD might have been blocked. Lastly, down-regulating FoxO1 using siFoxO1 also hindered the roles of KD in DCs (Fig. S8D-F). We also found that 740 Y-P activated the phosphorylation of PI3K (Tyr458), AKT (Ser473), and FoxO1 (Ser256), while, KD treatment caused less phosphorylation of these molecules, and

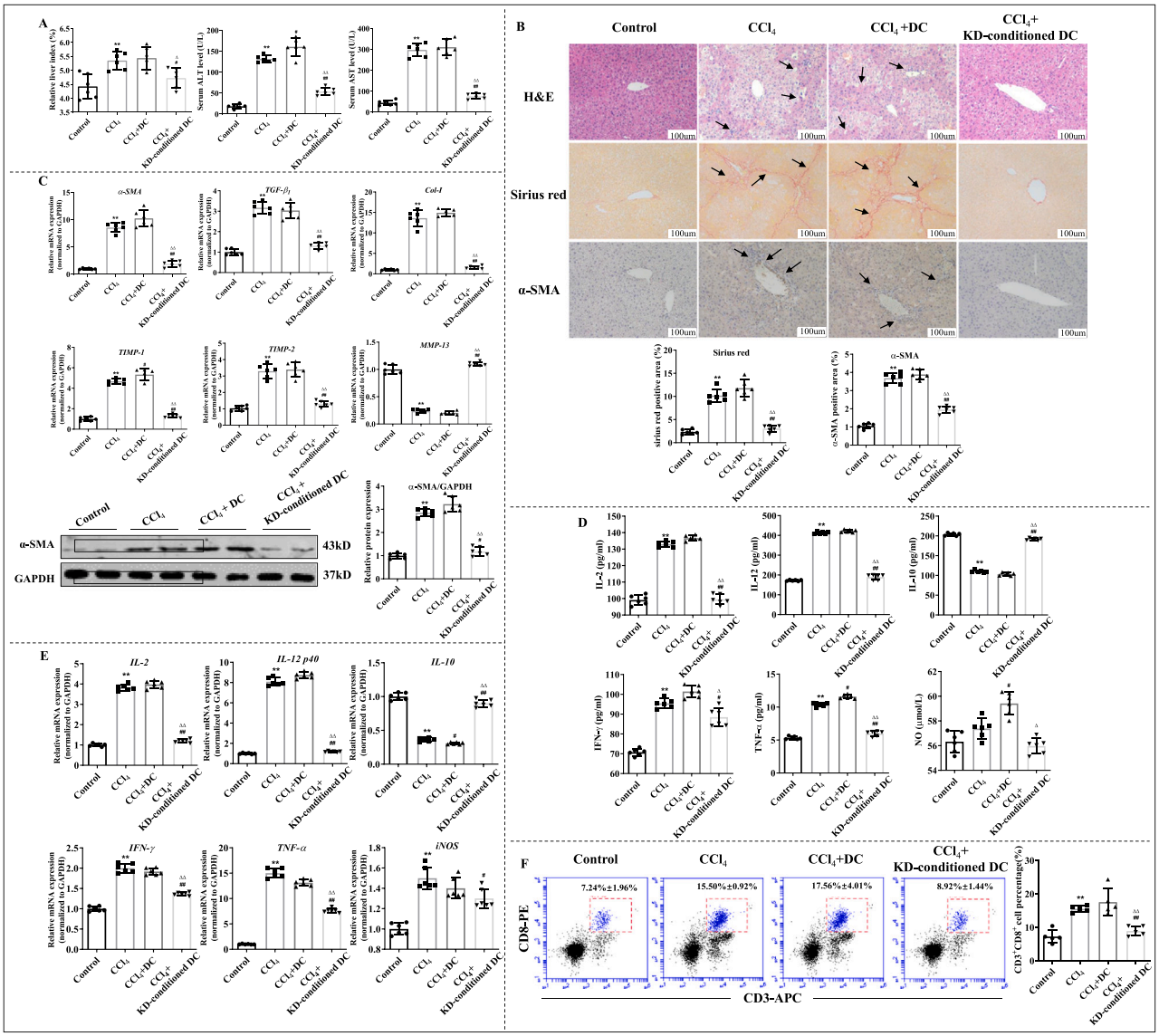

Fig. 4. KD-conditioned DCs alleviated CCl_4-induced LF and inhibited differentiation of $CD8^+$T cells. (A) Liver index and serum ALT and AST levels. (B) KD-conditioned DCs decreased LF severity. Representative images of H&E-, sirius red-, and α-SMA histochemical antibody (brown)- stained liver sections. Original magnification, × 200; scale bar, 100 μm. (C) Transcript levels of *α-SMA*, *TGF-β_1*, *Col-I*, *TIMP-1*, *TIMP-2*, and *MMP-13* and protein levels of α-SMA in the liver. (D) Serum inflammatory cytokine levels. (E) Hepatic inflammatory cytokine transcript levels. (F) Proportion of hepatic $CD8^+$T cells. Data expressed as mean ± SD (n = 6). $P < 0.01$ relative to controls; $^{\#}P < 0.05$, $^{\#\#}P < 0.01$ relative to CCl_4 group; $^{\Delta}P < 0.05$, $^{\Delta\Delta}P < 0.01$ relative to CCl_4+DC group.

increased FoxO1 presence in the nucleus of DCs (Fig. S9A and B). Interestingly, blockade of PI3K-AKT axis using LY294002 diminished the effect of KD on PI3K-AKT-FoxO1 axis (Fig. S9C and D), and PD-L1 expression on DCs (Fig. S8E and F).

To elucidate the mechanism whereby FoxO1 mediated the KD-induced immune tolerance of DCs, we further examined the direct interaction of FoxO1 and the PD-L1 promoter, using the ChIP assay. Based on our data, KD significantly increased FoxO1 binding to the PD-L1 promoter in LPS-activated DCs (Fig. 5 F). Collectively, these data reveals that KD antagonizes the stimulation of the PI3K-AKT axis in DCs followed by enhancing the interaction of FoxO1 with the PD-L1 promoter. These effects appear to be essential for the immunosuppressive actions of KD on inflammatory LF. Inhibitory effects of KD on immunogenic DCs are predominantly mediated by the PI3K-AKT axis.

3.6. KD suppressed HSC activation mediated by reducing IL-12 in DCs

Inhibiting the activation and ECM secretion of HSCs is the center for treating LF[40]. In addition, HSCs are capable of interacting with immune cells[41]. And it is considered that the activated immune cells-secreted IL-6/IL-12 cytokine family may be crucial for the activation of HSCs[42]. To further clarify the DC-induced HSC responses, we co-cultured JS-1 with DCs using transwell. The results demonstrated that treatment with BMDCs from LF mice increased the mRNA or/and protein level of α-SMA, Col-I, TGF-β_1 and TIMP-1 in JS-1, whereas the same treatment with KD-conditioned DCs reversed the upregulation of the aforementioned genes. Moreover, downregulation of IL-12 in DCs via siRNA transfection blocked the DC-mediated activation of JS-1. After blocking IL-12 expression, KD effect was also diminishing. On the contrary, IL-12 supplement reversed the effect of KD (Fig. 6). These data suggested that KD inhibited IL-12 generation in DCs, which impeded the interaction of JS-1 with DCs, thus reducing JS-1 activation.

Our data also revealed that both KD and LY294002 inhibited the expression and secretion of IL-12 in BMDCs, and the KD-mediated effect on IL-12 secretion was abolished upon pretreatment with PI3K inhibitor (Fig. 3 C and D, S4B and C, and S8F). Additionally, 740 Y-P raised IL-12

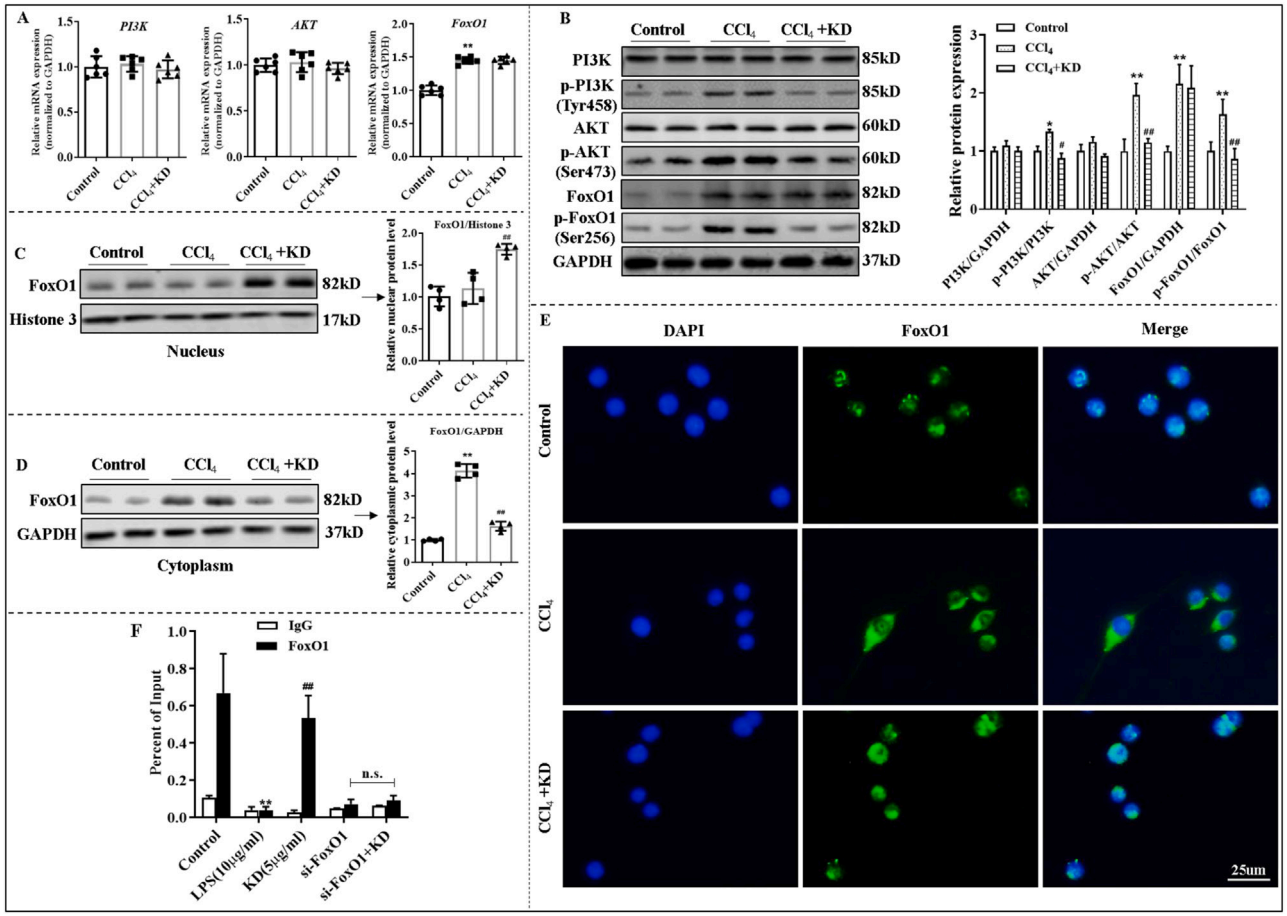

Fig. 5. KD modulated DC function via the PI3K-AKT-FoxO1 axis in DCs. (A) Transcript levels of *PI3K*, *AKT*, and *FoxO1* in DCs. (B) Total and phosphorylated levels of PI3K, AKT, and FoxO1 proteins of DCs. (C) Levels of nuclear FoxO1 protein of DCs. (D) Levels of cytoplasmic FoxO1 protein of DCs. (E) Immunofluorescence of FoxO1 (green) in DCs. BMDCs isolated from control mice or LF mice treated with or without KD (30 mg/kg). (F) ChIP assay exploring the physical binding between FoxO1 and PD-L1 promoter in DCs. IgG was used as the matched control. LPS-stimulated DCs were either exposed to KD (5 μg/mL) or not. Data expressed as mean ± SD (n = 6). $^{*}P < 0.05$, $^{**}P < 0.01$ relative to controls; $^{\#}P < 0.05$, $^{\#\#}P < 0.01$ relative to CCl_4 or LPS groups. n.s., not significant.

production in DCs, whereas KD reversed it (Fig. S8C). Furthermore, FoxO1 deficiency invalidated KD-mediated regulation of IL-12 generation by BMDCs (Fig. S8F). These results elucidated that the decreased expression and release of IL-12 in DCs by KD might rely on PI3K-AKT-FoxO1 axis.

4. Discussion

Herein, we demonstrated a KD-mediated suppressive effect on fibro-inflammation and DC function in CCl_4-induced LF. KD impeded the maturation of DCs and caused immunosuppression by promoting the binding of FoxO1 to the PD-L1 promoter via the PI3K-AKT pathway. Subsequently, the immunosuppressive DCs suppressed the $CD8^+$T cell differentiation by inducing PD-L1 and down-regulated HSC activity via secreting fewer IL-12 (Fig. 7).

The liver gathers a large population of DCs which enter the liver as immature cells via the portal vein and continue to mature with the progression of LF[43]. Hepatic aggregation of free cholesterol also activates non-parenchymal cells like DCs and kupffer cells, which produces persistent inflammation and fibrosis[44]. Hepatic inflammation during LF is regulated by immune cells, especially DCs. In patients with advanced LF, liver-infiltrating $CD8^+$T cells are abundant, and are likely abnormally induced by activated DCs [45]. DCs-regulated liver immunity also plays a central role in the progress of LF. Abnormal DCs accelerate the development of fibrosis [46]. Inflammatory DCs, expressing CX3C chemokine receptor1 (CX3CR1), play a major role in inflammation in mice with liver injury and are associated with elevated TNF-α levels [46]. Results reported here indicated that KD had an indirect regulation on normal liver cells (AML-12). However, KD-exposed DCs exhibited immature phenotypes, decreased chemokine receptor CCR7 densities, increased PD-L1 levels, lowered secretion of pro-inflammatory cytokines, and suppression of T cell activation, especially $CD8^+$T cells, thus alleviating liver injury and fibro-inflammation. Furthermore, adoptive transferring KD-conditioned DCs ameliorated inflammation and LF, which suggests that DCs are the main target cells mediating the inhibited effect of KD on fibro-inflammation in murine LF.

HSCs are the most important cell type involved in LF [47]. In normal liver, HSCs exist in a quiescent non-proliferative state [48]. During acute and chronic liver injury, HSCs activate and transdifferentiate to MFB [49], which are the main source of collagens and other ECM proteins [50]. The activation of HSCs could be stimulated by inflammatory cytokines, such as IL-1 and IL-6 [51]. Previous study reported IL-6/IL-12 cytokine family was able to transform quiescent HSCs into MFB via inducing STAT1 and STAT3 phosphorylation [42]. IL-12 is involved in the interaction between DC and HSC potentially. DC-mediated liver inflammation is predominantly reliant on IL-12, which contributes to the progression of LF [52]. Reports showed that AKT inhibitor promoted FoxO1 activation and inhibited IL-12 secretion in macrophages, and thus exerted an anti-inflammatory effect [53]. The AKT-mediated regulation of FoxO1 accelerated the IL-12 response and might be related to HSC activation in LF. Here, we revealed that KD showed contrasting effects on murine HSCs in vitro and in vivo. The effect of KD

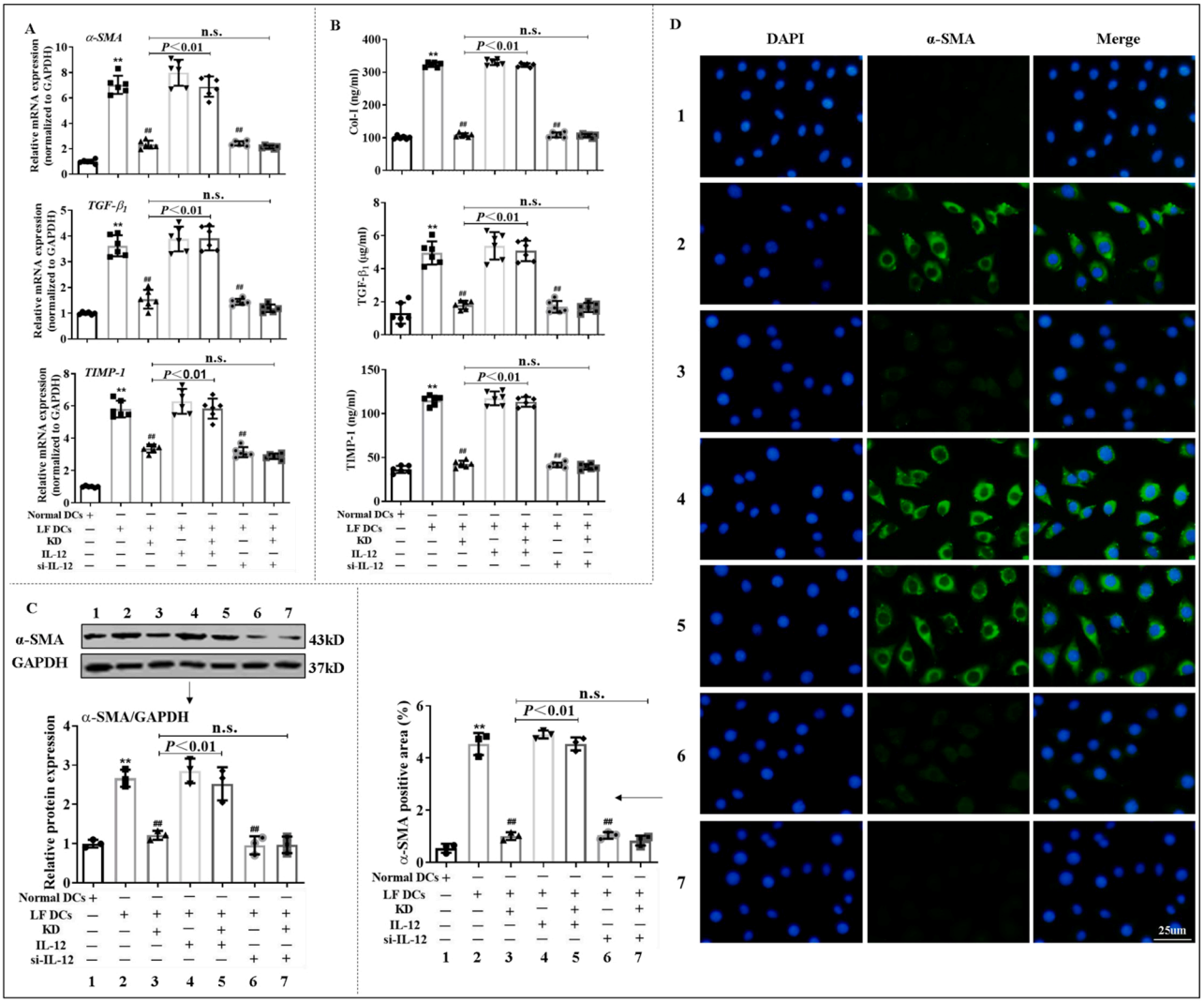

Fig. 6. KD inhibited DC cross-priming of HSC responses via reduction of IL-12 release from DCs. (A) Transcript levels of *α-SMA*, *TGF-β_1*, and *TIMP-1* in JS-1, as assessed by qPCR. (B) Extracellular secretion level of Col-I, TGF-β_1, and TIMP-1 in JS-1 tested by ELISA. (C-D) Protein levels of α-SMA in JS-1, as detected by WB and immunofluorescence. JS-1, with or without IL-12, was co-cultured with DCs isolated from normal or LF mice pre-treated with KD, si-IL-12, or KD+si-IL-12. Data expressed as mean ± SD (n = 6). $^{**}P < 0.01$ relative to normal DCs group; $^{\#\#}P < 0.01$ relative to LF DCs group. n.s., not significant.

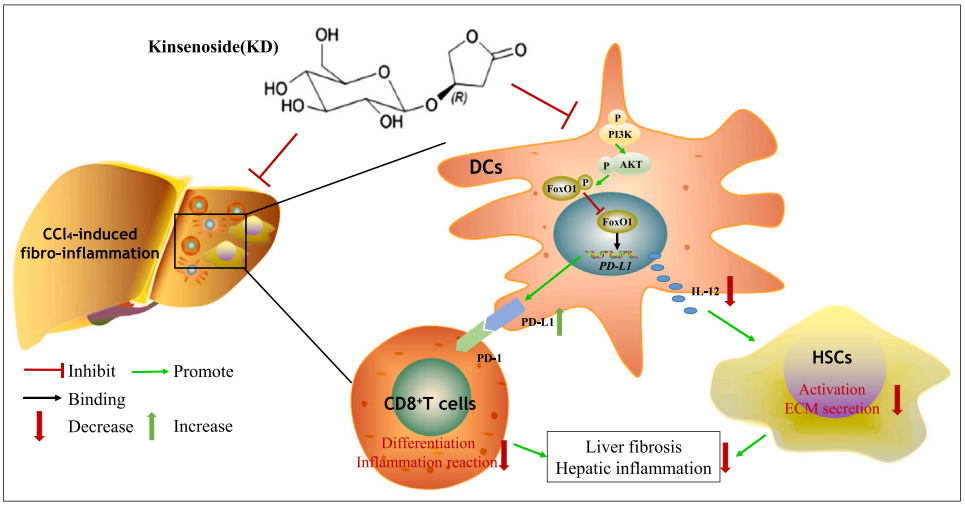

Fig. 7. A schematic diagram depicts the targets of KD in LF, involving PI3K-AKT-FoxO1-mediated regulation of DCs, and the interaction between DCs, $CD8^+$ T cells, and HSCs.

on HSCs required DC responsiveness. Furthermore, DCs amplified the KD effect on HSC by inhibiting IL-12 secretion of DCs. IL-12 deficiency in DCs suppressed the DC-stimulated activation of HSCs, and IL-12 supplement reversed the effect. KD reduced IL-12 secretion in DCs interrupted the pro-fibrotic interaction of hepatic DCs with HSCs.

The targeted effect of KD on fibrotic DCs might rely on PI3K-AKT axis in DCs. The PI3K-AKT axis regulates a myriad of cellular responses like cell survival, proliferation, metabolism, and so on [12,13]. Mice deficient in PI3K display severely impaired DC migration in response to the chemokines. In lymphocytes, PI3K are important in regulating basal lymphocyte motility, and PI3K expression is required for B cell morphology [54]. The PI3K-AKT axis participates in the reprogramming of the activities of numerous immune cells, especially DCs and macrophages [12]. PI3K-AKT axis was reported to be able to regulate the progression of acute lung injury via altering the maturation and function of DCs [14]. Additionally, the pathway is crucial for the glycolysis in DCs [55]. DC stimulation via toll-like receptor (TLR) agonists results in the acceleration of glycolysis. These alterations are produced by pathways that involves AKT, and are crucial for DC activation [56,57]. Additionally, targeted inhibition of AKT strongly suppresses the BMDCs capacity to react to TLR agonists and become stimulated [58]. Based on our results, the KD-mediated inhibition of the PI3K-AKT axis affected the MHC-II, CD86, CCR7 and IL-12 negatively, but PD-L1 and IL-10 positively in DC, which induced immunosuppression and suppressed hepatic damage in LF. KD also reversed the 740 Y-P (PI3K agonist)-mediated stimulation of the PI3K-AKT axis in DCs. Moreover, the LY294002 (PI3K antagonist) pretreatment inactivated the effects of KD, which was probably attributable to blocking the target of KD. As a consequence, PI3K-AKT axis might be a pivotal signal target for KD in DC of LF.

However, the molecular targets of PI3K-AKT in the regulation of DCs remain elusive. PI3K-AKT axis influences intracellular events via multiple pathways, for example, PI3K-AKT axis regulates cell survival and proliferation by activating metabolic genes sterol-regulatory element-binding proteins (SREBPs) and AS160[59,60]. Notably, FoxO1 is also a significant modulator of cell survival, metabolism and function[17]. AKT phosphorylates FoxO1 and causes FoxO1 to exit from the nucleus. In turn, it regulates the transcription of targeted genes [61]. In addition, FoxO1 facilitates cell cycle arrest partly via the production of cell cycle inhibitory agents like p27Kip1 and p21, and suppression of cyclin D1 levels [62]. Generally, the phosphorylation of the PI3K-AKT-FoxO1 axis is indispensable to the antigen presenting cells (APCs)-induced activation of T cells. Moreover, blocking the FoxO1 translocation to the cytoplasmic compartment can inhibit the expression of proliferation-associated genes in T cells [63]. During LF, activated AKT also phosphorylates FoxO1, which results in FoxO1 nuclear exit, and thus, transcriptions of the FoxO1-dependent genes p27kip1 and manganese superoxide dismutase (MnSOD) are negatively affected. P27kip1 silencing was shown to induce progression of HSCs into the S/G2/M phase of cell cycle and subsequent proliferation[64]. Our results showed that KD exposure could increase nuclear FoxO1 concentration and induce DC immunosuppression via FoxO1 interaction with the PD-L1 promoter. In contrast, siFoxO1-mediated FoxO1 deletion was competent to inhibit the KD-mediated effects on DCs. Targeting DCs and regulating PD-L1 promoter-FoxO1 combination by PI3K-AKT axis was important for KD effect on the protection against LF.

5. Conclusions

KD treatment improved the liver inflammatory microenvironment in LF and reprogrammed intracellular glycolysis to decrease DC migration and maturation. Mechanistically, KD diminished the activity of the PI3K-AKT axis and increased FoxO1 binding to the PD-L1 promoter. Thereby, KD promoted DC immunosuppression with the high PD-L1 and low IL-12, interrupted the interaction of hepatic DCs with $CD8^{+}$T cells or HSCs. Given the remarkable pharmacological activity and pharmacokinetic stability of KD, without other organ damages, and obvious non-toxicity, KD can serve as a new and efficient candidate for LF therapy.

CRediT authorship contribution statement

M.X. and Y.H.Z. participated in the study design, material support, coordination, and supervision of the study. T.T.L. and C.T. designed the experimental validation, performed experiments, analyzed the data, and drafted the manuscript. K.M., J.G., R.R.H., S.L.L., and Q.L. carried out parts of the experiments. C.R.X. and L.L gave techanical guidance. C.H.L provided constructive discussion about experiments. All authors read and approved the final manuscript.

Ethics approval and consent to participate

Animal care and experimental procedures were carried out in accordance with the guidelines of the Tongji Medical College, Huazhong University of Science and Technology Institutional Animal Care and Use Committee (IACUC Number: 2505).

Data availability

All data generated or analyzed during this study are included in this published article.

Funding

This work was supported by the National Natural Science Foundation of China [No. 82071749, 81903622, 81872000, 81673440, China]; the Key R&D Program of Hubei Province of China [No. 2020BHB019, China]; the Natural Science Foundation of Anhui Province of China [No. 1908085QH378, China]; the Program for HUST Interdisciplinary Innovation Team and the Fundamental Research Funds for the Central Universities [No. 2018KFYYXJJ022, China].

Declaration of Competing Interest

The authors declare that they have no known competing financial interests or personal relationships that could have appeared to influence the work reported in this paper.

Acknowledgements

We gratefully acknowledge Prof. Robert L. Rodgers, Department of Biomedical and Pharmaceutical Sciences, University of Rhode Island, for providing constructive discussions and language editing.

Appendix A. Supporting information

Supplementary data associated with this article can be found in the online version at doi:10.1016/j.phrs.2022.106092.

References

[1] X. Cai, J. Wang, J. Wang, Q. Zhou, B. Yang, Q. He, Q. Weng, Intercellular crosstalk of hepatic stellate cells in liver fibrosis: new insights into therapy, Pharm. Res 155 (2020), 104720, https://doi.org/10.1016/j.phrs.2020.104720.
[2] M.K. Connolly, A.S. Bedrosian, J. Mallen-St Clair, A.P. Mitchell, J. Ibrahim, A. Stroud, H.L. Pachter, D. Bar-Sagi, A.B. Frey, G. Miller, In liver fibrosis, dendritic cells govern hepatic inflammation in mice via TNF-alpha, J. Clin. Invest 119 (2009) 3213–3225, https://doi.org/10.1172/jci37581.
[3] L.W. Weber, M. Boll, A. Stampfl, Hepatotoxicity and mechanism of action of haloalkanes: carbon tetrachloride as a toxicological model, Crit. Rev. Toxicol. 33 (2003) 105–136, https://doi.org/10.1080/713611034.
[4] L. Campana, J.P. Iredale, Regression of liver fibrosis, Semin Liver Dis. 37 (2017) 1–10, https://doi.org/10.1055/s-0036-1597816.
[5] M. Parola, M. Pinzani, Liver fibrosis: pathophysiology, pathogenetic targets and clinical issues, Mol. Asp. Med 65 (2019) 37–55, https://doi.org/10.1016/j.mam.2018.09.002.
[6] Q. Miao, Z. Bian, R. Tang, H. Zhang, Q. Wang, S. Huang, X. Xiao, L. Shen, D. Qiu, E. L. Krawitt, M.E. Gershwin, X. Ma, Emperipolesis mediated by CD8 T cells is a

characteristic histopathologic feature of autoimmune hepatitis, Clin. Rev. Allergy Immunol. 48 (2015) 226–235, https://doi.org/10.1007/s12016-014-8432-0.
[7] H. Li, Y. Zhou, H. Wang, M. Zhang, P. Qiu, M. Zhang, R. Zhang, Q. Zhao, J. Liu, Crosstalk between liver macrophages and surrounding cells in nonalcoholic steatohepatitis, Front Immunol. 11 (2020) 1169, https://doi.org/10.3389/fimmu.2020.01169.
[8] L.J. Song, X.R. Yin, S.S. Mu, J.H. Li, H. Gao, Y. Zhang, P.P. Dong, C.J. Mei, Z. C. Hua, The differential and dynamic progression of hepatic inflammation and immune responses during liver fibrosis induced by schistosoma japonicum or carbon tetrachloride in mice, Front Immunol. 11 (2020), 570524, https://doi.org/10.3389/fimmu.2020.570524.
[9] Y. Xu, X. Tang, M. Yang, S. Zhang, S. Li, Y. Chen, M. Liu, Y. Guo, M. Lu, Interleukin 10 gene-modified bone marrow-derived dendritic cells attenuate liver fibrosis in mice by inducing regulatory T cells and inhibiting the TGF-β/Smad signaling pathway, Mediat. Inflamm. 2019 (2019) 4652596, https://doi.org/10.1155/2019/4652596.
[10] Y. Mi, J. Han, J. Zhu, T. Jin, Role of the PD-1/PD-L1 signaling in multiple sclerosis and experimental autoimmune encephalomyelitis: recent insights and future directions, Mol. Neurobiol. (2021), https://doi.org/10.1007/s12035-021-02495-7.
[11] M. Robert, P. Miossec, Reactivation of latent tuberculosis with TNF inhibitors: critical role of the beta 2 chain of the IL-12 receptor, Cell Mol. Immunol. 18 (2021) 1644–1651, https://doi.org/10.1038/s41423-021-00694-9.
[12] Y. Miao, M. Jiang, L. Qi, D. Yang, W. Xiao, F. Fang, BCAP regulates dendritic cell maturation through the dual-regulation of NF-κB and PI3K/AKT signaling during infection, Front Immunol. 11 (2020) 250, https://doi.org/10.3389/fimmu.2020.00250.
[13] X.J. Mi, J.G. Hou, S. Jiang, Z. Liu, S. Tang, X.X. Liu, Y.P. Wang, C. Chen, Z. Wang, W. Li, Maltol mitigates thioacetamide-induced liver fibrosis through TGF-β1-mediated activation of PI3K/Akt signaling pathway, J. Agric. Food Chem. 67 (2019) 1392–1401, https://doi.org/10.1021/acs.jafc.8b05943.
[14] R. Li, X. Zou, H. Huang, Y. Yu, H. Zhang, P. Liu, S. Pan, Y. Ouyang, Y. Shang, HMGB1/PI3K/Akt/mTOR signaling participates in the pathological process of acute lung injury by regulating the maturation and function of dendritic cells, Front Immunol. 11 (2020) 1104, https://doi.org/10.3389/fimmu.2020.01104.
[15] T. Zhao, J. Wang, A. He, S. Wang, Y. Chen, J. Lu, J. Lv, S. Li, J. Wang, M. Qian, H. Li, X. Shen, Mebhydrolin ameliorates glucose homeostasis in type 2 diabetic mice by functioning as a selective FXR antagonist, Metabolism 119 (2021), 154771, https://doi.org/10.1016/j.metabol.2021.154771.
[16] J.P. Scallan, L.A. Knauer, H. Hou, J.A. Castorena-Gonzalez, M.J. Davis, Y. Yang, Foxo1 deletion promotes the growth of new lymphatic valves, J. Clin. Invest 131 (2021), e142341, https://doi.org/10.1172/jci142341.
[17] Z. Xin, Z. Ma, W. Hu, S. Jiang, Z. Yang, T. Li, F. Chen, G. Jia, Y. Yang, FOXO1/3: potential suppressors of fibrosis, Ageing Res Rev. 41 (2018) 42–52, https://doi.org/10.1016/j.arr.2017.11.002.
[18] G. Dong, Y. Wang, W. Xiao, S. Pacios Pujado, F. Xu, C. Tian, E. Xiao, Y. Choi, D. T. Graves, FOXO1 regulates dendritic cell activity through ICAM-1 and CCR7, J. Immunol. 194 (2015) 3745–3755, https://doi.org/10.4049/jimmunol.1401754.
[19] H. Gao, L. Ding, R. Liu, X. Zheng, X. Xia, F. Wang, J. Qi, W. Tong, Y. Qiu, Characterization of Anoectochilus roxburghii polysaccharide and its therapeutic effect on type 2 diabetic mice, Int J. Biol. Macromol. 179 (2021) 259–269, https://doi.org/10.1016/j.ijbiomac.2021.02.217.
[20] C.C. Shih, Y.W. Wu, W.C. Lin, Antihyperglycaemic and anti-oxidant properties of Anoectochilus formosanus in diabetic rats, Clin. Exp. Pharm. Physiol. 29 (2002) 684–688, https://doi.org/10.1046/j.1440-1681.2002.03717.x.
[21] C.X. Qi, Q. Zhou, Z. Yuan, Z.W. Luo, C. Dai, H.C. Zhu, C.M. Chen, Y.B. Xue, J. P. Wang, Y.F. Wang, Y.P. Liu, M. Xiang, W.G. Sun, J.W. Zhang, Y.H. Zhang, Kinsenoside: a promising bioactive compound from anoectochilus species, Curr. Med Sci. 38 (2018) 11–18, https://doi.org/10.1007/s11596-018-1841-1.
[22] F. Zhou, J. Mei, X. Han, H. Li, S. Yang, M. Wang, L. Chu, H. Qiao, T. Tang, Kinsenoside attenuates osteoarthritis by repolarizing macrophages through inactivating NF-κB/MAPK signaling and protecting chondrocytes, Acta Pharm. Sin. B 9 (2019) 973–985, https://doi.org/10.1016/j.apsb.2019.01.015.
[23] K.T. Cheng, Y.S. Wang, H.C. Chou, C.C. Chang, C.K. Lee, S.H. Juan, Kinsenoside-mediated lipolysis through an AMPK-dependent pathway in C3H10T1/2 adipocytes: roles of AMPK and PPARα in the lipolytic effect of kinsenoside, Phytomedicine 22 (2015) 641–647, https://doi.org/10.1016/j.phymed.2015.04.001.
[24] X. Luo, S. Gu, Y. Zhang, J. Zhang, Kinsenoside ameliorates oxidative stress-induced RPE cell apoptosis and inhibits angiogenesis via Erk/p38/NF-κB/VEGF signaling, Front Pharm. 9 (2018) 240, https://doi.org/10.3389/fphar.2018.00240.
[25] Q. Liu, A.M. Qiao, L.T. Yi, Z.L. Liu, S.M. Sheng, Protection of kinsenoside against AGEs-induced endothelial dysfunction in human umbilical vein endothelial cells, Life Sci. 162 (2016) 102–107, https://doi.org/10.1016/j.lfs.2016.08.022.
[26] W.T. Hsieh, C.T. Tsai, J.B. Wu, H.B. Hsiao, L.C. Yang, W.C. Lin, Kinsenoside, a high yielding constituent from Anoectochilus formosanus, inhibits carbon tetrachloride induced Kupffer cells mediated liver damage, J. Ethnopharmacol. 135 (2011) 440–449, https://doi.org/10.1016/j.jep.2011.03.040.
[27] Y. Zhang, Y. Xia, Y. Lai, F. Tang, Z. Luo, Y. Xue, G. Yao, Y. Zhang, J. Zhang, Efficient synthesis of kinsenoside and goodyeroside a by a chemo-enzymatic approach, Molecules 19 (2014) 16950–16958, https://doi.org/10.3390/molecules191016950.
[28] Q. Wang, S. Wei, H. Zhou, L. Li, S. Zhou, C. Shi, Y. Shi, J. Qiu, L. Lu, MicroRNA-98 inhibits hepatic stellate cell activation and attenuates liver fibrosis by regulating HLF expression, Front Cell Dev. Biol. 8 (2020) 513, https://doi.org/10.3389/fcell.2020.00513.
[29] T. Liu, H. Cao, Y. Ji, Y. Pei, Z. Yu, Y. Quan, M. Xiang, Interaction of dendritic cells and T lymphocytes for the therapeutic effect of Dangguiliuhuang decoction to autoimmune diabetes, Sci. Rep. 5 (2015) 13982, https://doi.org/10.1038/srep13982.
[30] Z. Huang, M. Ding, Y. Dong, M. Ma, X. Song, Y. Liu, Z. Gao, H. Guan, Y. Chu, H. Feng, X. Wang, H. Liu, Targeted truncated TGF-beta receptor type II delivery to fibrotic liver by PDGFbeta receptor-binding peptide modification for improving the anti-fibrotic activity against hepatic fibrosis in vitro and in vivo, Int J. Biol. Macromol. 188 (2021) 941–949, https://doi.org/10.1016/j.ijbiomac.2021.08.055.
[31] M. Bartneck, C. Koppe, V. Fech, K.T. Warzecha, M. Kohlhepp, S. Huss, R. Weiskirchen, C. Trautwein, T. Luedde, F. Tacke, Roles of CCR2 and CCR5 for hepatic macrophage polarization in mice with liver parenchymal cell-specific NEMO deletion, Cell Mol. Gastroenterol. Hepatol. 11 (2021) 327–347, https://doi.org/10.1016/j.jcmgh.2020.08.012.
[32] Y. Tian, P. Shi, Y. Zhou, R. Yuan, Z. Hu, Y. Tan, G. Ma, L. Yang, H. Jiang, DiR-labeled tolerogenic dendritic cells for targeted imaging in collagen- induced arthritis rats, Int Immunopharmacol. 91 (2021), 107273, https://doi.org/10.1016/j.intimp.2020.107273.
[33] S. Wang, Z. Zhang, Q. Gao, Transfer of microRNA-25 by colorectal cancer cell-derived extracellular vesicles facilitates colorectal cancer development and metastasis, Mol. Ther. Nucleic Acids 23 (2021) 552–564, https://doi.org/10.1016/j.omtn.2020.11.018.
[34] L. Chen, R. Chen, S. Kemper, M. Cong, H. You, D.R. Brigstock, Therapeutic effects of serum extracellular vesicles in liver fibrosis, J. Extra Vesicles 7 (2018) 1461505, https://doi.org/10.1080/20013078.2018.1461505.
[35] J.A. Hill, T.E. Ichim, K.P. Kusznieruk, M. Li, X. Huang, X. Yan, R. Zhong, E. Cairns, D.A. Bell, W.P. Min, Immune modulation by silencing IL-12 production in dendritic cells using small interfering RNA, J. Immunol. 171 (2003) 691–696, https://doi.org/10.4049/jimmunol.171.2.691.
[36] S. Paccosi, L. Pala, B. Cresci, A. Silvano, M. Cecchi, R. Caporale, C. Maria Rotella, A. Parenti, Insulin resistance and obesity affect monocyte-derived dendritic cell phenotype and function, Diabetes Res Clin. Pr. 170 (2020), 108528, https://doi.org/10.1016/j.diabres.2020.108528.
[37] D. Pinheiro, I. Dias, K. Ribeiro Silva, A.C. Stumbo, A. Thole, E. Cortez, L. de Carvalho, R. Weiskirchen, S. Carvalho, Mechanisms underlying cell therapy in liver fibrosis: an overview, Cells 8 (2019) 1339, https://doi.org/10.3390/cells8111339.
[38] P. Giovanelli, T.A. Sandoval, J.R. Cubillos-Ruiz, Dendritic cell metabolism and function in tumors, Trends Immunol. 40 (2019) 699–718, https://doi.org/10.1016/j.it.2019.06.004.
[39] M. Xiang, T. Liu, W. Tan, H. Ren, H. Li, J. Liu, H. Cao, Q. Cheng, X. Liu, H. Zhu, Y. Tuo, J. Wang, Y. Zhang, Effects of kinsenoside, a potential immunosuppressive drug for autoimmune hepatitis, on dendritic cells/CD8(+) T cells communication in mice, Hepatology 64 (2016) 2135–2150, https://doi.org/10.1002/hep.28825.
[40] T.T. Liu, T.L. Ding, Y. Ma, W. Wei, Selective α1B- and α1D-adrenoceptor antagonists suppress noradrenaline-induced activation, proliferation and ECM secretion of rat hepatic stellate cells in vitro, Acta Pharm. Sin. 35 (2014) 1385–1392, https://doi.org/10.1038/aps.2014.84.
[41] M. Bomble, F. Tacke, L. Rink, E. Kovalenko, R. Weiskirchen, Analysis of antigen-presenting functionality of cultured rat hepatic stellate cells and transdifferentiated myofibroblasts, Biochem Biophys. Res Commun. 396 (2010) 342–347, https://doi.org/10.1016/j.bbrc.2010.04.094.
[42] C. Schoenherr, R. Weiskirchen, S. Haan, Interleukin-27 acts on hepatic stellate cells and induces signal transducer and activator of transcription 1-dependent responses, Cell Commun. Signal 8 (2010) 19, https://doi.org/10.1186/1478-811x-8-19.
[43] I.N. Crispe, Liver antigen-presenting cells, J. Hepatol. 54 (2011) 357–365, https://doi.org/10.1016/j.jhep.2010.10.005.
[44] K. Endo-Umeda, M. Makishima, Liver X receptors regulate cholesterol metabolism and immunity in hepatic nonparenchymal cells, Int J. Mol. Sci. 20 (2019) 5045, https://doi.org/10.3390/ijms20205045.
[45] M. Dudek, D. Pfister, S. Donakonda, P. Filpe, A. Schneider, M. Laschinger, D. Hartmann, N. Hüser, P. Meiser, F. Bayerl, D. Inverso, J. Wigger, M. Sebode, R. Öllinger, R. Rad, S. Hegenbarth, M. Anton, A. Guillot, A. Bowman, D. Heide, F. Müller, P. Ramadori, V. Leone, C. Garcia-Caceres, T. Gruber, G. Seifert, A. M. Kabat, J.P. Mallm, S. Reider, M. Effenberger, S. Roth, A.T. Billeter, B. Müller-Stich, E.J. Pearce, F. Koch-Nolte, R. Käser, H. Tilg, R. Thimme, T. Boettler, F. Tacke, J.F. Dufour, D. Haller, P.J. Murray, R. Heeren, D. Zehn, J.P. Böttcher, M. Heikenwälder, P.A. Knolle, Auto-aggressive CXCR6(+) CD8 T cells cause liver immune pathology in NASH, Nature 592 (2021) 444–449, https://doi.org/10.1038/s41586-021-03233-8.
[46] S. Sutti, I. Locatelli, S. Bruzzì, A. Jindal, M. Vacchiano, C. Bozzola, E. Albano, CX3CR1-expressing inflammatory dendritic cells contribute to the progression of steatohepatitis, Clin. Sci. (Lond.) 129 (2015) 797–808, https://doi.org/10.1042/cs20150053.
[47] Q. Hu, M. Liu, Y. You, G. Zhou, Y. Chen, H. Yuan, L. Xie, S. Han, K. Zhu, Dual inhibition of reactive oxygen species and spleen tyrosine kinase as a therapeutic strategy in liver fibrosis, Free Radic. Biol. Med 175 (2021) 193–205, https://doi.org/10.1016/j.freeradbiomed.2021.08.241.
[48] T. Tsuchida, S.L. Friedman, Mechanisms of hepatic stellate cell activation, Nat. Rev. Gastroenterol. Hepatol. 14 (2017) 397–411, https://doi.org/10.1038/nrgastro.2017.38.
[49] B. Dewidar, C. Meyer, S. Dooley, A.N. Meindl-Beinker, TGF-β in hepatic stellate cell activation and liver fibrogenesis-updated 2019, Cells (8() (2019), https://doi.org/10.3390/cells8111419.

[50] G.O. Elpek, Cellular and molecular mechanisms in the pathogenesis of liver fibrosis: an update, World J. Gastroenterol. 20 (2014) 7260–7276, https://doi.org/10.3748/wjg.v20.i23.7260.
[51] Z. Tan, H. Sun, T. Xue, C. Gan, H. Liu, Y. Xie, Y. Yao, T. Ye, Liver fibrosis: therapeutic targets and advances in drug therapy, Front Cell Dev. Biol. 9 (2021), 730176, https://doi.org/10.3389/fcell.2021.730176.
[52] T.C.M. Fontes-Cal, R.T. Mattos, N.I. Medeiros, B.F. Pinto, M. Belchior-Bezerra, B. Roque-Souza, W.O. Dutra, T.C.A. Ferrari, P.V.T. Vidigal, L.C. Faria, C.A. Couto, J.A.S. Gomes, Crosstalk between plasma cytokines, inflammation, and liver damage as a new strategy to monitoring NAFLD progression, Front Immunol. 12 (2021), 708959, https://doi.org/10.3389/fimmu.2021.708959.
[53] P. Gupta, S. Srivastav, S. Saha, P.K. Das, A. Ukil, Leishmania donovani inhibits macrophage apoptosis and pro-inflammatory response through AKT-mediated regulation of β-catenin and FOXO-1, Cell Death Differ. 23 (2016) 1815–1826, https://doi.org/10.1038/cdd.2016.101.
[54] J. Liu, X. Zhang, Y. Cheng, X. Cao, Dendritic cell migration in inflammation and immunity, Cell Mol. Immunol. (2021) 1–11, https://doi.org/10.1038/s41423-021-00726-4.
[55] I.S. Hansen, L. Krabbendam, J.H. Bernink, F. Loayza-Puch, W. Hoepel, J.A. van Burgsteden, E.C. Kuijper, C.J. Buskens, W.A. Bemelman, S.A.J. Zaat, R. Agami, G. Vidarsson, G.R. van den Brink, E.C. de Jong, M.E. Wildenberg, D.L.P. Baeten, B. Everts, J. den Dunnen, FcαRI co-stimulation converts human intestinal CD103(+) dendritic cells into pro-inflammatory cells through glycolytic reprogramming, Nat. Commun. 9 (2018) 863, https://doi.org/10.1038/s41467-018-03318-5.
[56] E.J. Pearce, B. Everts, Dendritic cell metabolism, Nat. Rev. Immunol. 15 (2015) 18–29, https://doi.org/10.1038/nri3771.
[57] S.L. Pompura, M. Dominguez-Villar, The PI3K/AKT signaling pathway in regulatory T-cell development, stability, and function, J. Leukoc. Biol. (2018), https://doi.org/10.1002/jlb.2mir0817-349r.
[58] B. Everts, E. Amiel, S.C. Huang, A.M. Smith, C.H. Chang, W.Y. Lam, V. Redmann, T. C. Freitas, J. Blagih, G.J. van der Windt, M.N. Artyomov, R.G. Jones, E.L. Pearce, E. J. Pearce, TLR-driven early glycolytic reprogramming via the kinases TBK1-IKKε supports the anabolic demands of dendritic cell activation, Nat. Immunol. 15 (2014) 323–332, https://doi.org/10.1038/ni.2833.
[59] J.R. Krycer, L.J. Sharpe, W. Luu, A.J. Brown, The Akt-SREBP nexus: cell signaling meets lipid metabolism, Trends Endocrinol. Metab. 21 (2010) 268–276, https://doi.org/10.1016/j.tem.2010.01.001.
[60] D. Baus, K. Heermeier, M. De Hoop, C. Metz-Weidmann, J. Gassenhuber, W. Dittrich, S. Welte, N. Tennagels, Identification of a novel AS160 splice variant that regulates GLUT4 translocation and glucose-uptake in rat muscle cells, Cell Signal 20 (2008) 2237–2246, https://doi.org/10.1016/j.cellsig.2008.08.010.
[61] J. Brown, H. Wang, J. Suttles, D.T. Graves, M. Martin, Mammalian target of rapamycin complex 2 (mTORC2) negatively regulates Toll-like receptor 4-mediated inflammatory response via FoxO1, J. Biol. Chem. 286 (2011) 44295–44305, https://doi.org/10.1074/jbc.M111.258053.
[62] F. Seiler, J. Hellberg, P.M. Lepper, A. Kamyschnikow, C. Herr, M. Bischoff, F. Langer, H.J. Schäfers, F. Lammert, M.D. Menger, R. Bals, C. Beisswenger, FOXO transcription factors regulate innate immune mechanisms in respiratory epithelial cells, J. Immunol. 190 (2013) 1603–1613, https://doi.org/10.4049/jimmunol.1200596.
[63] S. Fabre, V. Lang, J. Harriague, A. Jobart, T.G. Unterman, A. Trautmann, G. Bismuth, Stable activation of phosphatidylinositol 3-kinase in the T cell immunological synapse stimulates Akt signaling to FoxO1 nuclear exclusion and cell growth control, J. Immunol. 174 (2005) 4161–4171, https://doi.org/10.4049/jimmunol.174.7.4161.
[64] M. Adachi, Y. Osawa, H. Uchinami, T. Kitamura, D. Accili, D.A. Brenner, The forkhead transcription factor FoxO1 regulates proliferation and transdifferentiation of hepatic stellate cells, Gastroenterology 132 (2007) 1434–1446, https://doi.org/10.1053/j.gastro.2007.01.033.